Distribution of lipid aldehydes in phase-separated membranes : a molecular dynamics study

Distribution of Lipid Aldehydes in Phase-separated Membranes: A Molecular Dynamics Study

Maria C. Oliveira[†,‡], Maksudbek Yusupov[†,§], Annemie Bogaerts[†], Rodrigo M. Cordeiro[‡*]

[†]Research Group PLASMANT, Department of Chemistry, University of Antwerp, Universiteitsplein 1, B-2610 Antwerp, Belgium

[‡]Centro de Ciências Naturais e Humanas, Universidade Federal do ABC, Avenida dos Estados 5001, CEP 09210-580 Santo André, SP, Brazil

[§]Laboratory of Thermal Physics of Multiphase Systems, Arifov Institute of Ion-Plasma and Laser Technologies, Academy of Sciences of Uzbekistan, Durmon yuli str. 33, 100125, Tashkent, Uzbekistan

*corresponding author: rodrigo.cordeiro@ufabc.edu.br

ABSTRACT

It is well established that lipid aldehydes (LAs) are able to increase the permeability of cell membranes and induce their rupture. However, it is not yet clear how LAs are distributed in phase-separated membranes (PSMs), which are responsible for the transport of selected molecules and intracellular signaling. Thus, we investigate here the distribution of LAs in a PSM by coarse-grained molecular dynamics simulations. Our results reveal that LAs derived from mono-unsaturated lipids tend to accumulate at the interface between the liquid-ordered/liquid-disordered domains, whereas those derived from poly-unsaturated lipids remain in the liquid-disordered domain. These results are important for understanding the effects caused by oxidized lipids in membrane structure, properties and organization.

Keywords: lipid aldehydes, membrane permeability, phase-separated membranes, molecular dynamics simulations.

INTRODUCTION

Membranes of eukaryotic cells are important, e.g., for protecting the cells and acting as transporters of biomolecules into the cell interior [1]. Nowadays, it is well established that lipid membranes can be separated into nano- or microdomains, usually referred to as “lipid rafts” [2,3], which play a role in many biological processes. Such processes are for instance, numerous signal transduction pathways, apoptosis, cell adhesion and migration, synaptic transmission, organization of the cytoskeleton and protein sorting during both exocytosis and endocytosis [4-6]. Lipid rafts consist of liquid-ordered (Lo) and liquid-disordered (Ld) phases, where the former is mainly composed of saturated lipids (or sphingolipids) and cholesterol (Lo), and the latter is mainly composed of unsaturated lipids (Ld) [7,8]. Experimentally, lipid rafts have proven difficult to visualize in living cell membranes, and the degree of phase-separation remains unknown due to the similarity in the constituents and structures of the lipids [9-11].

Studies have shown that cholesterol plays an important role in lipid rafts formation. For instance, Krause and co-workers experimentally demonstrated that cholesterol is pushed away from low-melting (unsaturated) lipids and pulled towards high-melting (saturated) lipids (i.e., push-pull mechanism) [12]. This means that cholesterol exhibits attractive interactions in the Lo phase and repulsive interactions in the Ld phase. A few years later, Wang et al., showed that these repulsive interactions can be much stronger than the attractive interactions [13]. In another study, it was observed that the overload of cholesterol in neurodegenerative diseases leads to an increased partitioning of beta-amyloid proteins into lipid rafts, resulting in an increased amyloid formation and contributing to the progress of the neurodegenerative disease [14].

Computer simulations have proven to be powerful tools to describe the lipid phase-separation in membranes [15-17]. However, atomistic details of phase-separation in membranes are still a challenge due to slow lateral diffusion of lipids, compared to the typical timescales of computer simulations (nano- to microseconds) [18]. To bypass the long simulation times required to observe lipid phase-separation, membranes with pre-formed coexisting phases (domains) can be used (see e.g., [19]). Alternatively, coarse-grained (CG) models are able to

access larger length and timescales compared to atomistic simulations [20-22]. Marrink et al. developed a CG force field for biomolecular systems, known as the Martini force field, which is based on the mapping of four heavy (non-hydrogen) atoms into one bead [23,24]. In this way, the degrees of freedom can be decreased and the time step to integrate the Newton's equations of motion can be 1 to 2 orders of magnitude larger than in atomistic simulations, thus allowing the investigation of larger systems over longer timescales. A number of CG models using the Martini force field have been used to investigate the phase-separation in multicomponent membranes [25-27]. In some of these works, the authors investigated the mechanisms that explain phase-separation in three-component [25,26] and four-component [27] lipid mixtures.

Although extensive efforts have been performed to understand the behavior of phase-separated membranes (PSMs), there still remain several open questions. During the last decades, a number of experimental and computational studies have been devoted to understand the mechanisms and effects of lipid oxidation in cell membranes, which can be correlated with inflammatory, cancer and neurodegenerative diseases [28-31]. For instance, Wiczew and co-workers showed that a small area of a cell membrane (with or without cholesterol) oxidized into aldehydes (lipid aldehydes (LAs)) would induce the formation of wide enough pores (up to ~5 nm diameter) to transport ions and large molecules [32]. However, the effect of lipid oxidation on a PSM (with lipid rafts) as well as the interfacial activity of lipids at the domain boundaries, still need to be elucidated. Previously, we showed that the addition of a few LAs at the interface between domains is able to increase the membrane permeability up to 3-fold [19]. These results suggest that interfaces between PSMs are regions where pore formation is facilitated, inducing cell death either directly or as a consequence of membrane rupture.

To confirm our earlier assumption that LAs have actually a tendency to accumulate at domain interfaces, in the present study we performed CG molecular dynamics (MD) simulations to investigate the phase-separation in a membrane, as well as the lateral diffusion of LAs in this PSM, over a long simulation time. Since membrane lipids can also interact with several membrane proteins [33-35], oxidized lipids have been linked to protein aggregation and amyloid formation of disordered proteins, involved in type-II diabetes, Alzheimer’s

and Parkinson's diseases [36], anxiety and depression [37] and schizophrenia [38]. Thus, this study may be of interest for understanding the membrane damage caused by lipid oxidation in cancer cells, during for instance photodynamic therapy (PDT), cold atmospheric plasma (CAP), as well as in diabetes and neurodegenerative disorders.

METHODS

Preparation of the CG Models

We built the CG models using the *insane* (*INSert membrANE*) tool [39]. Although phase-separation has been experimentally observed in ternary mixtures of DPPC (1,2-dipalmitoyl-*sn*-glycero-3-phosphocholine) / ChL (cholesterol) / DOPC (1,2-dioleoyl-*sn*-glycero-3-phosphatidylcholine) [40-42], and DPPC/ChL/POPC (1-palmitoyl-2-oleoyl-*sn*-glycero-3-phosphocholine) [43,44], the current Martini force field is unable to reproduce phase-separation of these mixtures [25,45]. This limitation is intrinsic to the force field parametrization, which was parametrized to reproduce experimental densities of water and some alkanes at room temperatures. However, it tends to underestimate conformational entropy of the system, and some parts of the interaction are incorporated as enthalpic energy. This feature opened the question whether conformations play a role in the phase separation of ternary mixtures described by the Martini force field. Interestingly, CG MD simulations of ternary mixtures of DPPC/ChL/DOPC and DPPC/ChL/DAPC (1,2-diarachidoyl-*sn*-glycero-3-phosphocholine) indicated that the phase-separation within the Martini force field is primarily driven by interactions between hydrophobic tail beads, rather than structural/conformational differences between DPPC and unsaturated PC molecules [25].

One way to solve that limitation is the use of temperatures that are below experimental phase-separation, or the use of lipids with a higher level of unsaturation. For example, ternary mixtures of poly-unsaturated lipids such as DPPC/ChL/DIPC (1,2-dilinoleoyl-*sn*-glycero-3-phosphocholine) and DPPC/ChL/DAPC were used in CG MD simulations to reproduce phase-separation [46,47]. Thus, we studied phase-separation in a CG model membrane that contains (randomly distributed) 256 DIPC lipids, 256 DPPC lipids and 128

ChL molecules, together with 11012 water molecules surrounding them in the top and bottom layers (ca. 21 water molecules per lipid molecule). The molecular structures of all lipid molecules used in our CG MD simulations are presented in Figure 1.

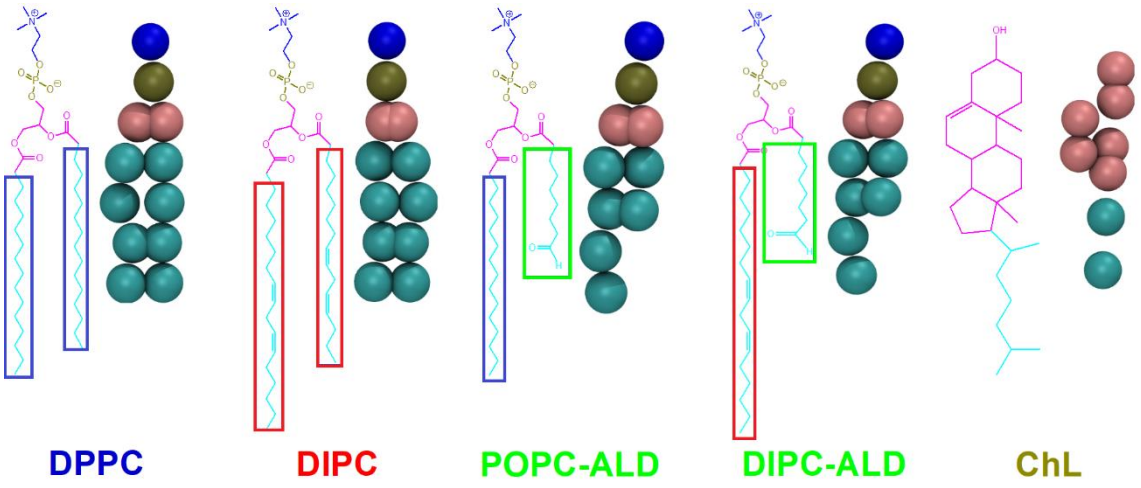

Figure 1. Molecular structures of the lipids (DPPC, DIPC, POPC-ALD, DIPC-ALD) and cholesterol (ChL) molecules, and mapping of four heavy (non-hydrogen) atoms into one bead, for use in our CG MD simulations. Blue, dark yellow, pink and cyan colors represent the choline, phosphate, glycerol groups and acyl chains, respectively. The rectangles in red, blue and green represent unsaturated (chain A), saturated (chain B) and oxidized chains of the lipids, respectively.

We applied the GROMACS version 2020.2 [48] in combination with the Martini v2.0 force field [24] in its standard (nonpolarizable) water model. After energy minimization of the model system, we performed the equilibration for 12 μs with a time step of 30 fs. The temperature was maintained at 310 K using the velocity-rescaling thermostat [49], with relaxation time of 1.0 ps. The system was semi-isotropically coupled to the Parrinello-Rahman barostat [50] to maintain its pressure at 1 bar. The pressure in the *xy* plane was kept equal to that in the *z* direction, with relaxation time of 12.0 ps and compressibility of 3×10^{-4} bar^{-1}, in line with those values used in earlier membrane simulations performed with the Martini force field [51-53]. In principle, larger values of compressibility should facilitate fluctuations in the membrane area, but they are not expected to affect average equilibrium properties. Electrostatic interactions were explicitly calculated within a cut-off of 1.1 nm with a relative dielectric constant of 15.

Beyond this cut-off, the interactions were computed by the reaction-field method [54], with an infinitely large dielectric constant. We used periodic boundary conditions in all Cartesian directions. Topology parameters of all molecules were taken from the Martini force field [23,24] and are available in the Supporting Information (SI).

During the 12 μs equilibration, the phase-separation was achieved within 3 μs, yielding a system composed of two domains: Lo phase (DPPC + ChL molecules) and Ld phase (DIPC lipid molecules). The membrane remained stable until the end of the simulation (see Figure S1 in the SI).

After phase-separation, we replaced some lipids of the Ld domain randomly by LA molecules. Specifically, we studied two types of LAs: derived from either mono-unsaturated POPC (POPC-ALD) or poly-unsaturated DIPC (DIPC-ALD) lipids (see Figure 1). Each CG model membrane was composed of 256 DPPC lipids, 204 DIPC lipids, 52 LAs (i.e., 10% of the total lipids), 128 ChL molecules and 11012 water molecules. Similar to the native system, the CG model membranes with 10% LAs were equilibrated for 12 μs, at the same conditions mentioned above. Note that we adjusted the Martini force field parameters of the POPC and DIPC lipids to build in the parameters of the POPC-ALD and DIPC-ALD lipids. The topology files of these molecules can be found in the SI.

In order to check whether our CG parameters for LAs were in agreement with all-atom (AA) simulations, which (as suggested by the name) account for all individual atoms, and are thus not bound by the assumptions of the CG approach, we also performed CG simulations using membranes (or bilayers) consisting of (1) 100% POPC-ALD lipids and (2) 25% POPC-ALD lipids and 75% POPC lipids. At AA level, Boonnoy and co-workers observed full pore formation in the bilayer consisting entirely of LAs [55]. At 50% oxidation with LAs, the pores were stable. However, at 100% of LAs the pores became unstable and micellation occurred within 1 μs [55]. In agreement with [55], we observed no pore formation in our CG model with 25% POPC-ALD lipids, even after 10 μs of simulation (Figure S2). On the other hand, again in agreement with [55], we observed pore formation at around 18 ns of simulation with 100% POPC-ALD (Figure S3). These results indicate that our simulations with CG parameters for LAs correspond well with the AA simulations. We also calculated the angle distributions of both models to

correlate the AA and CG model systems. To compare both, we converted the topology of a AA model to a CG model, using the *backward* tool [56], and we performed a CG simulation. As is clear from Figure S4, the angle variation of both simulations was similar.

Visualization and Data Analysis

Visualization of the CG and atomistic models was carried out using the VMD software [57]. We used the *gmx density* and *gmx rdf* tools of GROMACS for analysis of the mass density and radial distribution function of the lipids, respectively. Furthermore, we used the FATSLiM software [58] to calculate the two-dimensional distribution of the area per lipid and the bilayer thickness (for each domain).

RESULTS AND DISCUSSION

In our previous work, we hypothesized that LAs prefer to concentrate at domain interfaces, which leads to a stronger permeabilization effect. Our results showed that only a few LAs at the interface between the Lo/Ld domains were enough to increase the membrane permeability [19]. In the present study, we performed CG MD simulations, adding randomly the LAs at the Ld domain, in order to see if they indeed tend to accumulate at the interface between the Lo/Ld domains after a long timescale. As discussed in the methodology section, we simulated two LA-derivatives: one derived from mono-unsaturated POPC lipids (POPC-ALD) and another derived from poly-unsaturated DIPC lipids (DIPC-ALD). Interestingly, the POPC-ALD lipids accumulated at the interface after 6 μs of simulation (Figure 2A), but the same did not occur for DIPC-ALD lipids, even after 12 μs (Figure 2B). These results are corroborated by the density profiles (Figure 3): we can note a higher density of POPC-ALD lipids at the interface between the Lo/Ld domain (see Figure 3A), while the DIPC-ALD lipids remained at the Ld domain (see Figure 3B). It is noteworthy that there was no pore formation in either case.

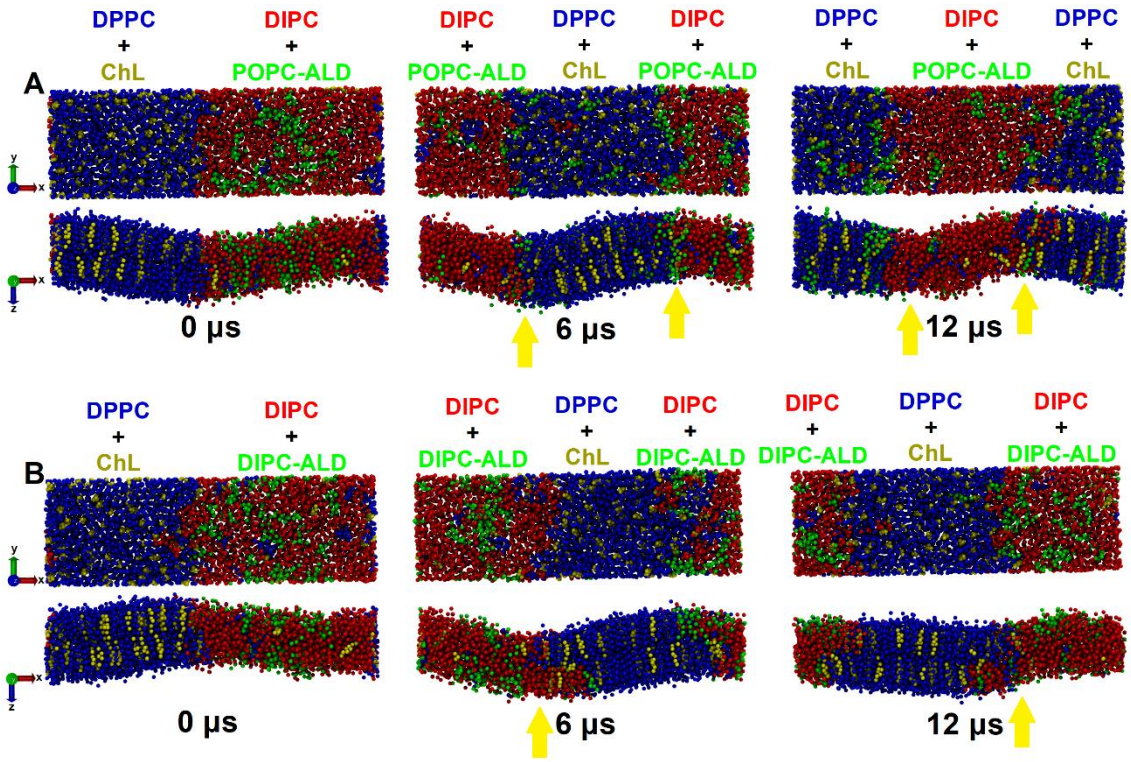

Figure 2. Top view (upper panels) and side view (bottom panels) of the CG model membranes, where the Ld domain is composed either of (**A**) DIPC and POPC-ALD lipids or (**B**) DIPC and DIPC-ALD lipids. The Lo domain in both cases is composed of DPPC + ChL. Each bead is represented as a van der Waals sphere. Water molecules are not shown for the sake of clarity. The accumulation of POPC-ALD lipids at the interface after 6 and 12 µs of simulation in case (**A**) is indicated by the green van der Waals spheres, while in case (**B**) the DIPC-ALD lipids stay in the Ld domain, as also indicated by the green van der Waals spheres. Yellow arrows indicate the membrane constriction regions.

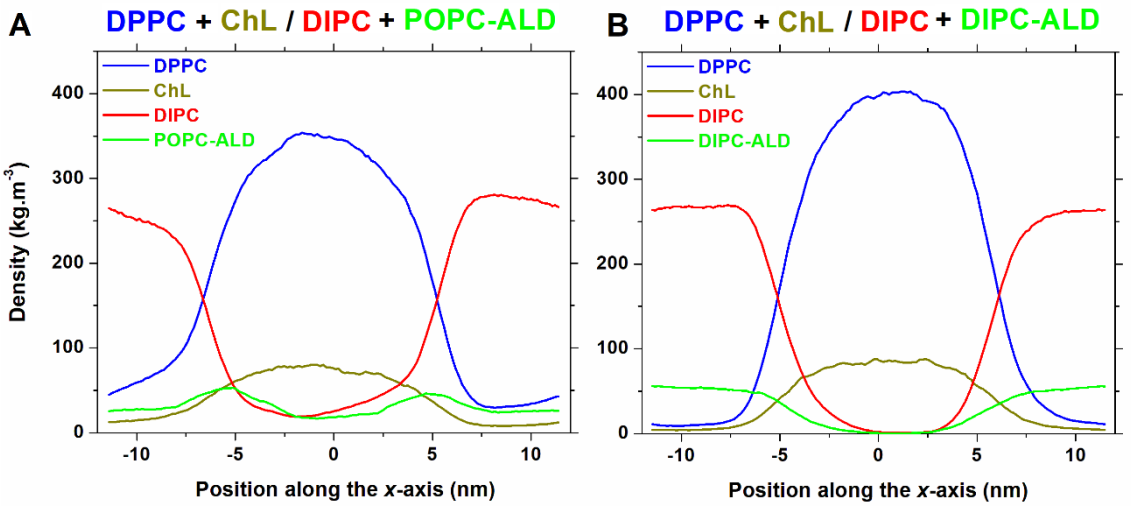

Figure 3. Density profile of the CG model membranes, where the Ld domain is composed either of (**A**) DIPC and POPC-ALD lipids or (**B**) DIPC and DIPC-ALD lipids. The accumulation of POPC-ALD lipids at the Ld/Lo interface is clear from the maximum in the density profile (around -5 and +5 nm) (**A**), while no maximum at the interface is observed for the DIPC-ALD lipids (**B**). The values were calculated from the last 6 μs of simulations. The position $x = 0$ corresponds to the center of the Lo (DPPC + ChL) domain.

In addition, the presence of both POPC-ALD and DIPC-ALD did increase the area per lipid at (or around) the interface region (see red circles in Figure 4), inducing a membrane constriction (see Figure 2). It is in agreement with our previous study, where we observed an increase of the local membrane curvature upon addition of POPC-ALD [19]. An increase of the area per lipid leads to a decrease of the bilayer thickness and a lower density in the membrane interior, thereby facilitating pore formation.

The temporal evolution of the area per lipid is shown in Figures S5 and S6 in SI. As is clear, in both systems, we can see a rise in the area per lipid at 12 μs. The truncated and highly mobile tails of the LAs have been proven to act as a water transporter, forming a bilayer thickness minimum in the oxidized region [59,60]. Indeed, we observed that the bilayer thickness of the Ld domain was smaller in the presence of LAs (see Figure S7). All together, these features of LAs increase the membrane susceptibility to fluctuations and subsequent pore formation.

We observed that when the intact (i.e., non-oxidized) lipid chain is saturated (i.e., LA-derived from POPC), it tends to accumulate at the interface, whereas it remains at the Ld domain when it is unsaturated (i.e., LA-derived from DIPC). This suggests that the interfacial activity is driven by the interactions between saturated (POPC-ALD) and unsaturated (DIPC-ALD) lipid acyl chains of the LAs with the Lo (POPC + ChL) and Ld (DIPC) domains. Indeed, a systematic study with the Martini force field has shown that phase separation is primarily driven by differences in van der Waals interactions between saturated and unsaturated fragments [25].

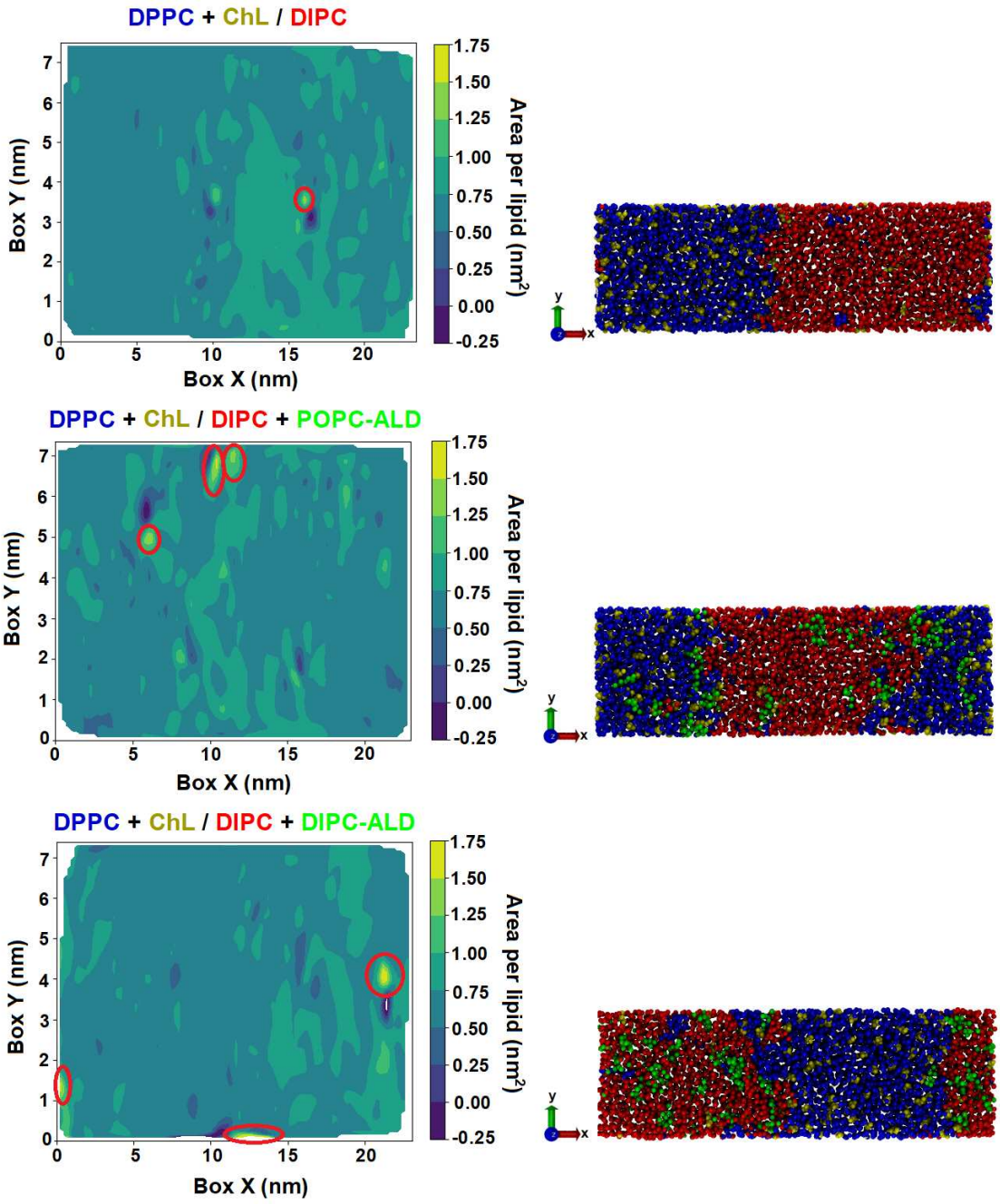

Figure 4. Two-dimensional distribution of the area per lipid calculated at 12 μs of simulation (top view of only a single MD frame) (left side). Red circles indicate the positions where the area per lipid is higher. The right side also represents a top view of the membrane, but in this case the lipids are explicit. The box sizes in *x* and *y*-axes are the same in the right and left sides, but they are represented in different scales.

We also performed atomistic simulations using the same lipid composition of the CG model membranes, to evaluate whether significant changes take place in the atomistic (AA) model system, i.e., the model system which better represents a real system. We found that the simulation time (10 μs) used in our

AA simulations was insufficient for POPC-ALD and DIPC-ALD lipids to diffuse laterally to the membrane interface and accumulate there (or not) (see Figures S8 and S9). It was found in another simulation study that the lateral diffusion coefficients for phospholipids were in the order of ~ 0.01 $nm^2.ns^{-1}$ [61], which indicates that in 10 μs, a completely random lateral motion of an individual lipid would be limited to within a circle with a radius smaller than 6 nm. This is too small compared to the membrane size used in our simulations (i.e., ~ 17 nm in the *x* direction). Thus, these low lipid lateral diffusion coefficients require longer simulation time than used in our AA simulations (i.e., longer than 10 μs). Our AA simulations showed more bending close to the interface region in the DPPC + ChL / DIPC + DIPC-ALD system, i.e., a higher thickness mismatch between the Lo and Ld domains (see Figure 5 and Table S1). As a consequence, the membrane might be more susceptible to pore formation at the interface region, although this was not observed in neither AA model. Nevertheless, our CG models reproduce well the structural properties of the AA models (see Table S1), although the dynamics in the CG model are of course faster than that of the AA model, which are because of the fewer degrees of freedom of the atoms in the CG model.

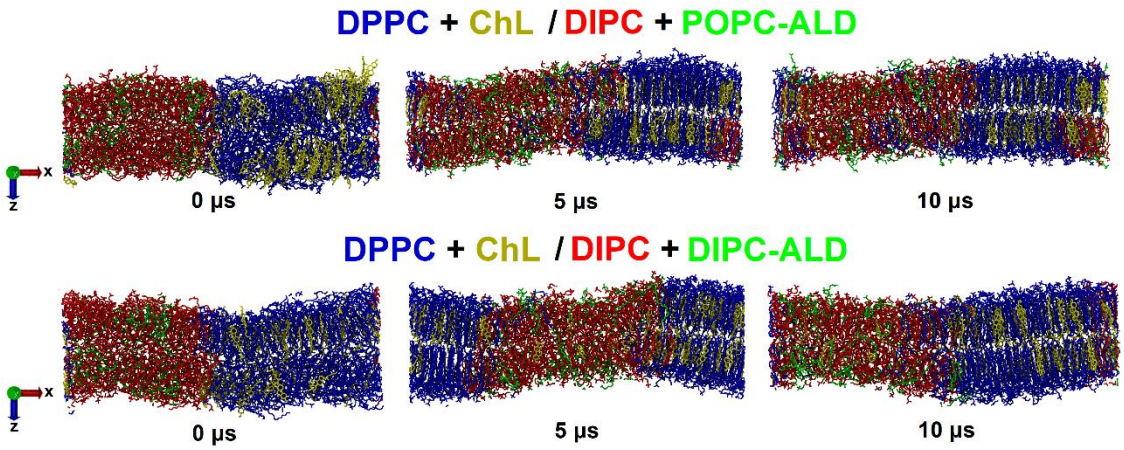

Figure 5. Side view of the atomistic model membranes, where the Ld domain is composed either of DIPC and POPC-ALD lipids (upper panels) or DIPC and DIPC-ALD lipids (bottom panels). The Lo domain in both cases is composed of DPPC + ChL. Lipid molecules are represented as solid lines. Water molecules are not shown for the sake of clarity.

To summarize, we hypothesize that the saturated acyl chains of POPC-ALD interact with the saturated acyl chains of DPPC lipids [31], so that they

accumulate at the interface between the Lo/Ld domains, since the truncated (oxidized) chains of POPC-ALD interact with unsaturated chains of DIPC. Likewise, the unsaturated acyl chains of DIPC-ALD interact with the unsaturated acyl chains of DIPC lipids, and with the truncated (oxidized) chains of DIPC-ALD, therefore they remain in the Ld domain. This hypothesis is corroborated by calculation of the radial distribution function (RDF) for the oxidized, unsaturated (chain A) and saturated (chain B) acyl chains of POPC-ALD and DIPC-ALD, with the unsaturated (chain A) and saturated (chain B) acyl chains of DIPC and DPPC lipids, respectively (see Figure 1). Indeed, as shown in Figure 6A, the probability density to find a chain at a distance of 0.5 nm from the oxidized chain of POPC-ALD is higher for chain A of DIPC than for chain B of DPPC, whereas the probability density to find a chain at 0.5 nm from the chain B of POPC-ALD is the same for both chain A and chain B of DIPC and DPPC, respectively. Likewise, the probability density to find a chain at a distance of 0.5 nm from either the oxidized or chain A of DIPC-ALD is higher for chain A of DIPC than for chain B of DPPC (Figure 6B).

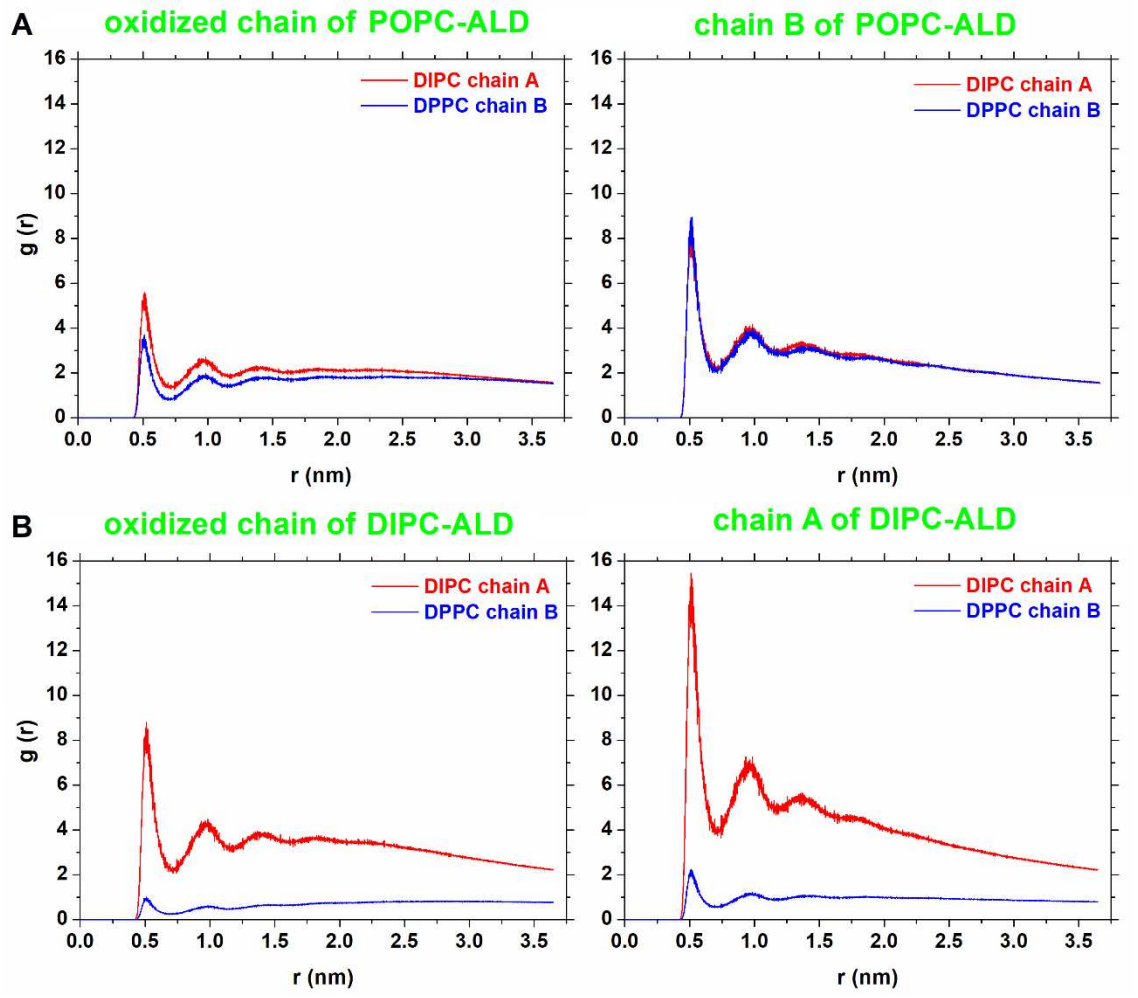

Figure 6. Radial distribution function calculated for oxidized chains of POPC-ALD and DIPC-ALD from the last 6 μs of simulation. Chains A and B represent unsaturated and saturated chains, respectively. The values for chains A and B were calculated as an average between the two chains A or B of each lipid type.

Overall, not only oxidized acyl chains affect the distribution of LAs in PSMs, but also the structure of the lipids (saturation or unsaturation) plays a role. Although the timescale of our (very expensive) atomistic simulations (10 μs) was not enough to show the distribution of the LAs at the interfaces, our CG results seem realistic to describe their preference of accumulation in a PSM.

CONCLUSIONS

We performed CG MD simulations to evaluate the distribution of LAs in PSMs. Our results reveal that LAs derived from mono-unsaturated lipids (POPC-ALD) tend to accumulate at the interface between the Lo/Ld domains.

Conversely, LAs derived from poly-unsaturated lipids (DIPC-ALD) tend to remain in the Ld domain. These investigations help to elucidate how LAs, which are well-known membrane lipid oxidation products that increase the membrane permeability, can be distributed in complex membrane systems. These insights can be important for understanding the molecular level mechanisms of membrane damage caused by lipid oxidation and its role in membrane structure, properties and organization. For instance, our findings can be relevant for plasma application in medicine, to target and disrupt regions prone to pore formation in cancer cell membranes.

ACKNOWLEDGMENTS

We thank the University of Antwerp and the Coordination of Superior Level Staff Improvement (CAPES, Brazil) for the scholarship granted. The calculations were performed using the Turing HPC infrastructure at the CalcUA core facility of the Universiteit Antwerpen (UAntwerpen), a division of the Flemish Supercomputer Center VSC, funded by the Hercules Foundation, the Flemish Government (department EWI) and the UAntwerpen.

REFERENCES

[1] M. S. Bretscher, *Membrane structure: some general principles*, Science 181 (1973) 622-629.

[2] K. Simons and E. Ikonen, *Functional rafts in cell membranes*, Nature 387 (1997) 569-572.

[3] D. Lingwood and K. Simons, *Lipid Rafts as a Membrane-Organizing Principle*, Science 327 (2010) 46-50.

[4] T. K. Nyholm, *Lipid-protein interplay and lateral organization in biomembranes*, Chem. Phys. Lipids 189 (2015) 48-55.

[5] E. Sezgin, I. Levental, S. Mayor, C. Eggeling, *The mystery of membrane organization: composition, regulation and roles of lipid rafts*, Nat. Rev. Mol. Cell Biol. 18 (2017) 361-374.

[6] E. J. Miller, A. M. Ratajczak, A. A. Anthony, M. Mottau, X. I. R. Gonzalez, A. R. Honerkamp-Smith, *Divide and conquer: How phase separation contributes to lateral transport and organization of membrane proteins and lipids*, Chem. Phys. Lipids 233 (2020) 104985.

[7] S. L. Veatch and S. L. Keller, *Organization in lipid membranes containing cholesterol*, Phys. Rev. Lett. 89 (2002) 268101.

[8] A. J. Sodt, M. L. Sandar, K. Gawrisch, R. W. Pastor, E. Lyman, R. W. Pastor, *The Molecular Structure of the Liquid Ordered Phase of Lipid Bilayers*, J. Am. Chem. Soc. 136 (2014) 725-732.

[9] I. H. Lee, S. Saha, A. Polley, H. Huang, S. Mayor, M. Rao, J. T. Groves, *Live Cell Plasma Membranes Do Not Exhibit a Miscibility Phase Transition over a Wide Range of Temperatures*, J. Phys. Chem. B 119 (2015) 4450-4459.

[10] M. G. Tian, Y. Liu, Y. M. Sun, R. Y. Zhang, R. Q. Feng, G. Zhang, L. F. Guo, X. C. Li, X. Q. Yu, J. Z. Sun, X. Q. He, *A single fluorescent probe enables clearly discriminating and simultaneously imaging liquid-ordered and liquid-disordered microdomains in plasma membrane of living cells*, Biomaterials 120 (2017) 46-56.

[11] T. Tsuji T. and Fujimoto, *Lipids and lipid domains of the yeast vacuole*, Biochem. Soc. Trans. 46 (2018) 1047-1054.

[12] M. R. Krause, T. A. Daly, P. F. Almeida, S. L. Regen, *Push-Pull Mechanism for Lipid Raft Formation*, Langmuir 30 (2014) 3285-3289.

[13] C. Wang, Y-M. Yu, S. L. Regen, *Lipid Raft Formation: Key Role of Polyunsaturated Phospholipids*, Angew. Chem., Int. Ed. 56 (2017) 1639-1642.

[14] M. Kosicek, M. Malnar, A. Goate, S. Hecimovic, *Cholesterol accumulation in Niemann Pick type C (NPC) model cells causes a shift in APP localization to lipid rafts*, Biochem. Biophys. Res. Commun. 393 (2010) 404-409.

[15] D. Duque, *Particle method for phase separation on membranes*, Microfluidics and Nanofluidic 22 (2018) 95.

[16] R-X. Gu, S. Baoukina, D. P. Tieleman, *Phase Separation in Atomistic Simulations of Model Membranes*, J. Am. Chem. Soc. 142 (2020) 2844-2856.

[17] A. Fathizadeh, M. Valentine, C. R. Baiz, R. Elber, *Phase Transition in a Heterogeneous Membrane: Atomically Detailed Picture*, J. Phys. Chem. Lett. 11 (2020) 5263-5267.

[18] J. S. Allhusen and J. C. Conboy, *The Ins and Outs of Lipid Flip-flop*, Acc. Chem. Res. 50 (2017) 58-65.

[19] M. C. Oliveira, M. Yusupov, A. Bogaerts, R. M. Cordeiro, *Lipid Oxidation: Role of Membrane Phase-Separated Domains*, J. Chem. Inf. Model. 61 (2021) 2857-2868.

[20] C. Hong, D. P. Tieleman, Y. Wang, *Microsecond Molecular Dynamics Simulations of Lipid Mixing*, Langmuir 30 (2014) 11993-12001.

[21] H. Koldsø, M. S. P. Sansom, *Organization and Dynamics of Receptor Proteins in a Plasma Membrane*, J. Am. Chem. Soc. 137 (2015) 14694-14704.

[22] H. Koldsø, T. Reddy, P. W. Fowler, A. L. Duncan, M. S. P. Sansom, *Membrane Compartmentalization Reducing the Mobility of Lipids and Proteins within a Model Plasma Membrane*, J. Phys. Chem. B 120 (2016) 8873-8881.

[23] S. J. Marrink, A. H. de Vries, A. E. Mark, *Coarse Grained Model for Semi-Quantitative Lipid Simulations*, J. Phys. Chem. B 108 (2004) 750-760.

[24] S. J. Marrink, H. J. Risselada, S. Yefimov, D. P. Tieleman, A. H. de Vries, *The MARTINI force field: coarse grained model for biomolecular simulations*, J. Phys. Chem. B 111 (2007) 7812-7824.

[25] R. S. Davis, P. B. S. Kumar, M. M. Sperotto, M. Laradji, *Predictions of Phase Separation in Three-Component Lipid Membranes by the MARTINI Force Field*, J. Phys. Chem. B 117 (2013) 4072-4080.

[26] G. A. Pantelopulos and J. E. Straub, *Regimes of Complex Lipid Bilayer Phases Induced by Cholesterol Concentration in MD Simulation*, Biophys. J. 115 (2018) 2167-2178.

[27] D. G. Ackerman and G. W. Feigenson, *Multiscale Modeling of Four-Component Lipid Mixtures: Domain Composition, Size, Alignment, and Properties of the Phase Interface*, J. Phys. Chem. B 119 (2015) 4240-4250.

[28] M. A. Bradley-Whitman, M. A. Lovell, *Biomarkers of Lipid Peroxidation in Alzheimer Disease (AD): an update*, Arch. Toxicol. 89 (2015) 1035-1044.

[29] M. Yusupov, K. Wende, S. Kupsch, E. C. Neyts, S. Reuter, A. Bogaerts, *Effect of head group and lipid tail oxidation in the cell membrane revealed through integrated simulations and experiments*, Sci. Rep. 7 (2017) 5761.

[30] R. Munir, J. Lisec, J. V. Swinnen, N. Zaidi, *Lipid Metabolism in Cancer Cells under Metabolic Stress*, Br. J. Cancer 120 (2019) 1090-1098.

[31] J. Van der Paal, S-H. Hong, M. Yusupov, N. Gaur, J-S. Oh, R. D. Short, E. J. Szili, A. Bogaerts, *How membrane lipids influence plasma delivery of reactive oxygen species into cells and subsequent DNA damage: an experimental and computational study*, Phys. Chem. Chem. Phys. 21 (2019) 19327-19341.

[32] D. Wiczew, N. Szulc, M. Tarek, *Molecular dynamics simulations of the effects of lipid oxidation on the permeability of cell membranes*, Biolectrochem. 141 (2021) 107869.

[33] B. J. Reynwar and M. Deserno, *Membrane composition-mediated protein-protein interactions*, Biointerphases 3 (2008) FA117-FA124.

[34] C. La Rosa, S. Scalisi, F. Lolicato, M. Pannuzzo, A. Raudino, *Lipid-assisted protein transport: A diffusion-reaction model supported by kinetic experiments and molecular dynamics simulations*, J. Chem. Phys. 144 (2016) 184901.

[35] F. Scollo, C. Tempra, F. Lolicato, M. F. M. Sciacca, A. Raudino, D. Milardi, C. La Rosa, *Phospholipids Critical Micellar Concentrations Trigger Different Mechanisms of Intrinsically Disordered Proteins Interaction with Model Membranes*, J. Phys. Chem. Lett. 9 (2018) 5125-5129.

[36] M. F. Sciacca, F. Lolicato, C. Tempra, F. Scollo, B. R. Sahoo, M. D. Watson, S. García-Viñuales, D. Milardi, A. Raudino, J. C. Lee, A. Ramamoorthy, C. La Rosa, *Lipid-Chaperone Hypothesis: A Common Molecular Mechanism of Membrane Disruption by Intrinsically Disordered Proteins*, ACS Chem. Neurosci. 11 (2020) 4336-4350.

[37] A. G. Fedoce, F. Ferreira, R. G Bota, V. Bonet-Costa, P. Y. Sun, K. J. A. Davies, *The role of oxidative stress in anxiety disorder: cause or consequence?*, Free Radic. Res. 52 (2018) 737-750.

[38] Ö. K. Tunçel, G. Sarısoy, B. Bilgici, O. Pazvantoglu, E. Çetin, E. Ünverdi, B. Avcı, Ö. Böke, *Oxidative stress in bipolar and schizophrenia patients*, Psychiatry Res. 228 (2015) 688-694.

[39] T. A. Wassenaar, H. I. Ingolfsson, R. A. Böckmann, D. P. Tieleman, S. J. Marrink, *Computational Lipidomics with insane: A Versatile Tool for Generating Custom Membranes for Molecular Simulations*, J. Chem. Theory Comput. 11 (2015) 2144-2155.

[40] M. Yanagisawa, M. Imai, S. Komura, T. Ohta, *Growth Dynamics of Domains in Ternary Fluid Vesicles*, Biophys. J. 92 (2007)115-125.

[41] S. F. Shimobayashi, M. Ichikawa, T. Taniguchi, *Direct observations of transition dynamics from macro- to micro-phase separation in asymmetric lipid bilayers induced by externally added glycolipids*, EPL 113 (2016) 56005.

[42] N. Shimokawa, R. Mukai, M. Nagata, M. Takagi, *Formation of modulated phases and domain rigidification in fatty acid-containing lipid membranes*, Phys. Chem. Chem. Phys. 19 (2017) 13252-13263.

[43] A. Vogel, J. Nikolausa, K. Weise, G. Triola, H. Waldmann, R. Winter, A. Herrmann, D. Huster, *Interaction of the human N-Ras protein with lipid raft model membranes of varying degrees of complexity*, Biol. Chem. 395 (2014) 779-789.

[44] N. Q. Mei, M. Robinson, J. H. Davis, Z. Leonenko, *Melatonin Alters Fluid Phase Coexistence in POPC/DPP/Cholesterol Membranes*, Biophys. J. 119 (2020) 2391-2402.

[45] D. Hakobyan and A. Heuer, *Phase separation in a lipid/cholesterol system: comparison of coarse-grained and united-atom simulations*, J. Phys. Chem. B 117 (2013) 3841-3851.

[46] D. Hakobyan and A. Heuer, *Key molecular requirements for raft formation in lipid/cholesterol membranes*, PLoS One 9 (2014) e87369.

[47] S. Baoukina, D. Rozmanov, D. P. Tieleman, *Composition Fluctuations in Lipid Bilayers*, Biophys. J. 113 (2017) 2750-2761.

[48] M. J. Abraham, T. Murtola, R. Schulz, S. Pall, J. C. Smith, B. Hess, E. Lindahl, *GROMACS: High performance molecular simulations through multi-level parallelism from laptops to super-computers*, SoftwareX 1-2 (2015) 19-25.

[49] G. Bussi, D. Donadio, M. Parrinello, *Canonical sampling through velocity rescaling*, J. Chem. Phys. 126 (2007) 014101.

[50] M. Parrinello, A. Rahman, *Polymorphic Transitions in Single-Crystals - A new molecular-dynamics method*, J. Appl. Phys. 52 (1981) 7182-7190.

[51] C. Arnarez, J. J. Uusitalo, M. F. Masman, H. I. Ingolfsson, D. H. de Jong, M. N. Melo, X. Periole, A. H. de Vries, S. J. Marrink, *Dry Martini, a Coarse-Grained Force Field for Lipid Membrane Simulations with Implicit Solvent*, J. Chem. Theory Comput. 11 (2015) 260-275.

[52] Y. Guo, V. A. Baulina, F. Thalmann, *Peroxidised phospholipid bilayers: insight from coarse-grained molecular dynamics simulations*, Soft Matter 12 (2016) 263-271.

[53] T. S. Carpenter, C. A. Lopez, C. Neale, C. Montour, H. I. Ingolfsson, F. Di Natale, F. C. Lightstone, S. Gnanakaran, *Capturing Phase Behavior of Ternary Lipid Mixtures with a Refined Martini Coarse-Grained Force Field*, J. Chem. Theory Comput. 14 (2018) 6050-6062.

[54] A. Kubincová, S. Riniker, P. H Hünenberger, *Reaction-field electrostatics in molecular dynamics simulations: development of a conservative scheme compatible with an atomic cutoff*, Phys. Chem. Chem. Phys. 22 (2020) 26419-26437.

[55] P. Boonnoy, V. Jarerattanachat, M. Karttunen, J. Wong-ekkabut, *Bilayer Deformation, Pores, and Micellation Induced by Oxidized Lipids*, J. Phys. Chem. Lett. 6 (2015) 4884-4888.

[56] T. A. Wassenaar, K. Pluhackova, R. A. Böckmann, S. J. Marrink, D. P. Tieleman, *Going Backward: A Flexible Geometric Approach to Reverse Transformation from Coarse Grained to Atomistic Models*, J. Chem. Theory Comput. 10 (2014) 676-690.

[57] W. Humphrey, A. Dalke, K. Schulten, *VMD: Visual molecular dynamics*, J. Mol. Graphics 14 (1996) 33-38.

[58] S. Buchoux, *FATSLiM: a fast and robust software to analyze MD simulations of membranes*, Bioinformatics 33 (2017) 133-134.

[59] P. T. Vernier, Z. A. Levine, Y-H. Wu, V. Joubert, M. J. Ziegler, L. M. Mir, D. P. Peter Tieleman, *Electroporating Fields Target Oxidatively Damaged Areas in the Cell Membrane*, PLoS ONE 4 (2009) e7966.

[60] J. Van der Paal, E. C. Neyts, C. C. W. Verlackt, A. Bogarts, *Effect of Lipid Peroxidation on Membrane Permeability of Cancer and Normal Cells Subjected to Oxidative Stress*, Chem. Sci. 7 (2016) 489-498.

[61] A. Kukol, *Lipid Models for United-Atom Molecular Dynamics Simulations of Proteins*, J. Chem. Theory Comput. 5 (2009) 615-626.